Published OnlineFirst January 6, 2011; DOI: 10.1158/0008-5472.CAN-10-2700

E-3810 Is a Potent Dual Inhibitor of VEGFR and FGFR that Exerts Antitumor Activity in Multiple Preclinical Models

Ezia Bello[1], Gennaro Colella[2], Valentina Scarlato[1], Paolo Oliva[1], Alexander Berndt[3], Giovanni Valbusa[4], Sonia Colombo Serra[4], Maurizio D'Incalci[1], Ennio Cavalletti[2], Raffaella Giavazzi[1], Giovanna Damia[1], and Gabriella Camboni[2]

Abstract

Tumor angiogenesis is a degenerate process regulated by a complex network of proangiogenic factors. Existing antiangiogenic drugs used in clinic are characterized by selectivity for specific factors. Antiangiogenic properties might be improved in drugs that target multiple factors and thereby address the inherent mechanistic degeneracy in angiogenesis. Vascular endothelial growth factor (VEGF) and fibroblast growth factor (FGF) family members and their cognate receptors are key players in promoting tumor angiogenesis. Here we report the pharmacologic profile of E-3810, a novel dual inhibitor of the VEGF and FGF receptors. E-3810 potently and selectively inhibited VEGF receptor (VEGFR)-1, -2, and -3 and FGF receptor (FGFR)-1 and -2 kinases in the nanomolar range. Ligand-dependent phosphorylation of VEGFR-2 and FGFR-1 was suppressed along with human vascular endothelial cell growth at nanomolar concentrations. In contrast, E-3810 lacked cytotoxic effects on cancer cell lines under millimolar concentrations. In a variety of tumor xenograft models, including early- or late-stage subcutaneous and orthotopic models, E-3810 exhibited striking antitumor properties at well-tolerated oral doses administered daily. We found that E-3810 remained active in tumors rendered nonresponsive to the general kinase inhibitor sunitinib resulting from a previous cycle of sunitinib treatment. In Matrigel plug assays performed in nude mice, E-3810 inhibited basic FGF–induced angiogenesis and reduced blood vessel density as assessed by histologic analysis. Dynamic contrast-enhanced magnetic resonance imaging analysis confirmed that E-3810 reduced the distribution of angiogenesis-sensitive contrast agents after only 5 days of treatment. Taken together, our findings identify E-3810 as a potent antiangiogenic small molecule with a favorable pharmacokinetic profile and broad spectrum antitumor activity, providing a strong rationale for its clinical evaluation. *Cancer Res; 71(4); 1396–405. ©2011 AACR.*

Introduction

Cancer cell growth is dependent on neo-vascularization to deliver oxygen and nutrients (1, 2). The formation of new vessels relies on a complex series of orchestrated events with the activation of endothelial and perivascular cells (pericytes and smooth cells), and the modification of the surrounding basement membrane and extracellular matrix. Tumor angiogenesis is initiated by proangiogenic factors, produced by both host and tumor cells, including vascular endothelial growth factor (VEGF), platelet-derived growth factor (PDGF), fibroblast growth factor (FGF), angiopoietin, and others. VEGF, PDGF, and FGF act by binding to their cognate tyrosine kinase receptors on endothelial and stromal cells, setting in motion a cascade of intracellular signaling transduction pathways that leads to increased vascular permeability, endothelial and stromal cell survival and proliferation, invasion, and migration. This makes angiogenesis not only one of the hallmarks of cancers but also an important target for cancer therapy (3, 4).

Targeted agents are available that interfere with the formation and maintenance of blood vessels and can increase survival in cancer patients (5–7). These include bevacizumab, a monoclonal antibody to VEGF-A, as well as sunitinib, sorafenib, and pazopanib, small molecules with multitargeted tyrosine kinase inhibitory activity, encompassing activity against VEGF and PDGF receptors (VEGFR and PDGFR; refs 8–11). However, the clinical benefit induced by agents targeting the VEGF pathway is less than initially expected (12, 13). Several escape mechanisms have been shown in different preclinical models and may contribute to the disappointing clinical outcomes (14, 15). In particular, continuous VEGF blocking seems to activate alternative pathways (e.g., FGF/FGFR and PFGF/PDGFR) that drive angiogenesis and tumor progression (16–18).

Although the role of the FGF/FGFR pathway in tumor angiogenesis is established, the pathway is probably also

Authors' Affiliations: [1]Department of Oncology, Istituto di Ricerche Farmacologiche "Mario Negri," and [2]E.O.S. S.p.A., Milan; and [4]Centro Ricerche Bracco, Bracco Imaging S.p.A., Colleretto Giacosa (TO), Italy; [3]Institute of Pathology, University Hospital, Jena, Germany

Note: Supplementary data for this article are available at Cancer Research Online (http://cancerres.aacrjournals.org/).

Ezia Bello and Gennaro Colella contributed equally to this work.

Corresponding Author: Giovanna Damia, Istituto di Ricerche Farmacologiche "Mario Negri," Via La Masa 19, 20156 Milan, Italy. Phone: 39-02-39014473; Fax: 39-02-39014734; E-mail: giovanna.damia@marionegri.it

doi: 10.1158/0008-5472.CAN-10-2700

Published OnlineFirst January 6, 2011; DOI: 10.1158/0008-5472.CAN-10-2700

implicated in the development and maintenance of some solid and hematologic malignances (19–21). High FGF and FGFR expression levels have been reported in breast and prostate human cancers (22, 23). Experimental evidence suggests that FGFRs act as oncogenes in certain tumors and can act autonomously to maintain cancer cell growth (24, 25).

The possibility of hitting the FGF/FGFR pathways with the same molecule in tumor vasculature and in tumor cells might result in significant better therapeutic outcomes. A number of molecules that interfere with the FGF signal have been synthesized and are under investigation, including selective agents and molecules with a more complex kinase inhibition profile with activity against FGFR and other tyrosine kinase inhibitors, variably combined (24, 26).

We report here the pharmacologic characterization of E-3810, a novel dual inhibitor of VEGFR and FGFR. The compound is a very potent inhibitor of VEGFR and FGFR tyrosine kinases, is suitable for chronic oral administration, blocks FGF- and VEGF-driven angiogenesis, and shows broad antitumor activity *in vivo*, being active in all the human tumor xenografts tested. Tumors not responsive to sunitinb do respond to E-3810.

Materials and Methods

Cell cultures

Human umbelical vein cells (HUVEC) were isolated as described (27) and maintained as monolayer in MCDB131 medium supplemented with 20% (v/v) fetal bovine serum (FBS), 1% (v/v) L-glutammine, 5 units/mL heparin, and 50 μg/mL endothelial cell growth factor (ECGF) using culture flasks or plates precoated with 1% (v/v) gelatin. NIH3T3 (murine fibroblasts), A2780 (human ovarian carcinoma), A498 and SN12KI (human renal cancers), HepG2 (human hepatocarcinoma), and HT-29 (human colon carcinoma) cells were obtained from the American Type Culture Collection; RXF393 (human renal carcinoma) was obtained from Prof. H. Fiebig (Freiburg, Germany).

Drugs

E-3810, sunitinib, and brivanib were synthesized by ChemPartner Co. Ltd. All drugs were dissolved in 100% DMSO at a final concentration of 10 mM for *in vitro* treatment. For *in vivo* experiments drugs were dissolved in Methocel 0.5%; drug solutions were made every 5 days and kept at +4°C, as these working solutions are stable for at least 7 days, with the exception of brivanib, which was dissolved immediately before use. All treatments were administered by gavage daily at the doses and schedules described in the Results section of this article. B-B PDGF, $VEGF_{165}$, and basic FGF (bFGF) ligands were purchased from Peprotech (INALCO Spa).

Antiproliferative assays

Exponentially growing HUVEC or NHI3T3 cells were seeded into 96-well plates at a density of 3 to 6×10^3 cells/100 μL/well in complete medium. In the experiments without serum starvation, 24 hours after seeding, cells were exposed to different E-3810 concentrations without or with $VEGF_{165}$ (50 ng/mL) or bFGF (20 ng/mL) ligands and the antiproliferative effect of the drugs was evaluated after 72 hours by MTS Colorimetric Assay (Promega). In the assays with serum starvation conditions, 24 hours after seeding complete medium was removed and after 3 rounds of washing with PBS, cells were cultured in medium containing 1% BSA. After 18 to 24 hours, cells were processed as described earlier. Exponentially growing A2780, A498, SN12KI, and HepG2 cells were seeded into 96-well plates at 3 to 5×10^3 cells/100 μL/well in complete medium. Twenty-four hours later cells were treated with different drug concentrations for 72 hours and the antiproliferative effect was evaluated by MTS.

Xenograft models

Six- to eight-week-old female NCr-nu/nu mice were obtained from Harlan S.p.A., Italy. They were maintained under specific pathogen-free conditions, housed in isolated ventilated cages, and handled using aseptic procedures. Procedures involving animals and their care were conducted in conformity with institutional guidelines that are in compliance with national and international laws and policies. The procedures for subcutaneous and orthotopic implantation of the different tumors are specified in Supplementary Material and Methods. Tumor growth was measured twice weekly with a Vernier caliper, and tumor weights (mg = mm^3) were calculated as follows: (length [mm] × width $[mm]^2$)/2. Efficacy of the treatment was expressed as best tumor growth inhibition [$\%T/C$ = (median tumor weight of treated tumors/median tumor weight of control tumors) × 100] or tumor growth delay ($T - C$ = median time to reach 500 or 1000 mg in treated tumor − median time to reach 500 or 1000 mg in control tumor).

Immunohistochemistry

At the beginning ($T = 0$) and end of treatment ($T = 2$) representative mice from control and treated group were killed and tumors were excised and embedded in optimal cutting compound snap-frozen, and stored at −80°C. Cryosections (4 μm) were fixed in methanol/acetone at room temperature. Vessels were counted by immunostaining with anti-CD31 antibody MEC13.3 (Beckton Dickinson GmbH), followed by a biotin-conjugated mouse antirat IgG1/2a monoclonal antibody (clone G28-5, Beckton Dickinson GmbH), and a streptavidin-alkaline phosphatase (AP) conjugate (Biozol Diagnostika GmbH). Chromogenic detection was done with the chromogen solution of the Dako REAL Detection System AP/RED (Dako Deutschland GmbH). Three randomly selected measurement fields (0.57 mm^2) from each tumor with representative vessel density were scanned and the examiner marked all CD31-stained vascular structures. The vessel number was determined using computer-aided image analysis software (Axio Vision Release 4.6). For collagen type IV immunohistochemistry, cryosections were fixed with 4% paraformaldehyde for 15 minutes. Then the antimurine collagen type IV antibody AB756 (Millipore/Chemicon, Schwalbach/Ts.) was applied followed by biotin-SP-conjugated AffiniPure Goat anti Rabbit IgG(H+L) (Dianova GmbH). To assess the extent of collagen type IV staining, 3 randomly selected areas

Published OnlineFirst January 6, 2011; DOI: 10.1158/0008-5472.CAN-10-2700

($0.57\ mm^2$) of each tumor were captured photographically. The red stained area (representing collagen IV deposition) was assessed by computer-aided image analysis and as a percentage of the whole measurement area (Axio Vision Release 4.6). The necrotic tumor area was evaluated after H&E staining. Whole tumor sections were scanned at low power (4× objective = $3.58\ mm^2$ area). The examiner marked the total tumor area and the necrotic tumor area on the scanned microscopic images and the areas were calculated by computer-aided image analysis, giving the tumor necrosis area as a percentage of the total tumor area.

In vivo magnetic resonance imaging

Magnetic resonance imaging scans were performed on A498-bearing mice treated (3 mice) with E-3810 or not (2 mice) using a BioSpec AVIII system (Bruker BioSpin) dedicated to small rodents, equipped with a 7 Tesla/30-cm magnet and a 35-mm birdcage RF coil. All mice were imaged just before (T0) and 5 days (T1) and 12 days (T2) after daily vehicle and E-3810 treatment. Throughout the duration of the scans, animals were kept under controlled anesthesia (about 30% O_2, 70% N_2, and 0.8–1% isofluorane). Tumor vascularization was investigated by dynamic contrast enhanced (DCE) series comprising 74 transversal FLASH (Fast Low Angle SHot) 2-dimensional (2D) T_1 weighted scans acquired after injection of the contrast agent (CA) B22956/1 (Bracco Imaging SpA; ref. 28), 0.1 mmol/kg, with the following parameters: TR/TE 100/3.5 ms, flip angle (FA) 90°, matrix size 128 × 256, field-of-view 2.5 × 2.5 cm^2 (corresponding to ca. 200 × 100 μm^2 in-plane resolution), 6 slices 2 mm thick, acquisition time 59 seconds/image. One scan with the same parameters was run before CA injection. Precontrast T_1 values in tumors were measured using a multislice variable flip-angle FLASH (29). Image 2D reconstruction for all MRI experiments was done using the proprietary scanner software ParaVision. Image postprocessing and analysis were carried out by in-house developed routines running under ImageJ (Rasband W.S., NIH, http://rsbweb.nih.gov/ij/docs/faqs.html).

Statistical analyses

Statistical analyses for the evaluation of the antitumor activity were done using Prism software (Prism 5.01; GraphPad Software). Statistical differences were evaluated by 2-way ANOVA followed by Bonferroni's *post hoc* test. $P < 0.05$ was considered significant. Statistical analysis for the evaluation of the MRI experiments was done with SPSS (SPSS Inc., Rel. 17.0.0. 2008).

Results

In vitro studies

The chemical structure and physical properties of E-3810 (6-(7-((1-aminocyclopropyl) methoxy)-6-methoxyquinolin-4-yloxy)-N-methyl-1-naphthamide) are shown in Fig. 1. In initial screenings against panels of receptor and cytoplasmic kinases (Supplementary Table S1), E-3810 potently inhibited the tyrosine kinase activity of VEGF and FGF receptors. Table 1 shows the IC_{50} values on different receptor tyrosine kinases.

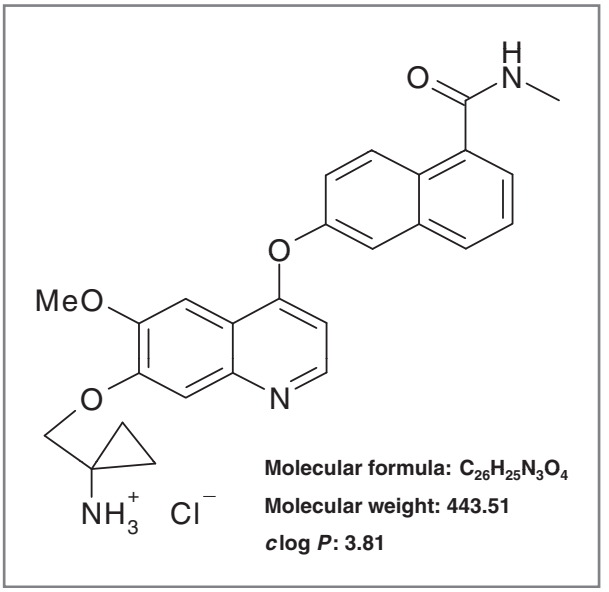

Figure 1. Chemical structure and physical properties of E-3810.

Selective activity was in the low- nanomolar range for VEGFR-1, -2, -3, FGFR-1, -2, and colony stimulating factor (CSF)-1R; the compound also had some activity against FGFR-3, PDGFR α, and PDGFR β, with 20 times lower potency.

The selectivity of E-3810 was preserved in cellular systems. HUVEC treatment with E-3810 in the low nanomolar range caused dose-dependent inhibition of the ligand-dependent phosphorylation of VEGFR-2 and FGFR-1 (Supplementary Fig. S1A and B). In the same experimental conditions, ERK

Table 1. *In vitro* kinase inhibition profile E-3810

Kinase	E-3810
	IC_{50} (nM)
VEGFR family	
VEGFR-1	7
VEGFR-2	25
VEGFR-3	10
FGFR family	
FGFR-1	17.5
FGFR-2	82.5
FGFR-3	237.5
FGFR-4	>1000
PDGFR family	
c-Kit	456
PDGFR α	175
PDGFR β	525
CSF-1R	5

NOTE: Assays were done with ATP concentrations at the respective K_m. IC_{50s}; >1000 means that half-maximum inhibition was not achieved at the highest concentration tested.

Published OnlineFirst January 6, 2011; DOI: 10.1158/0008-5472.CAN-10-2700

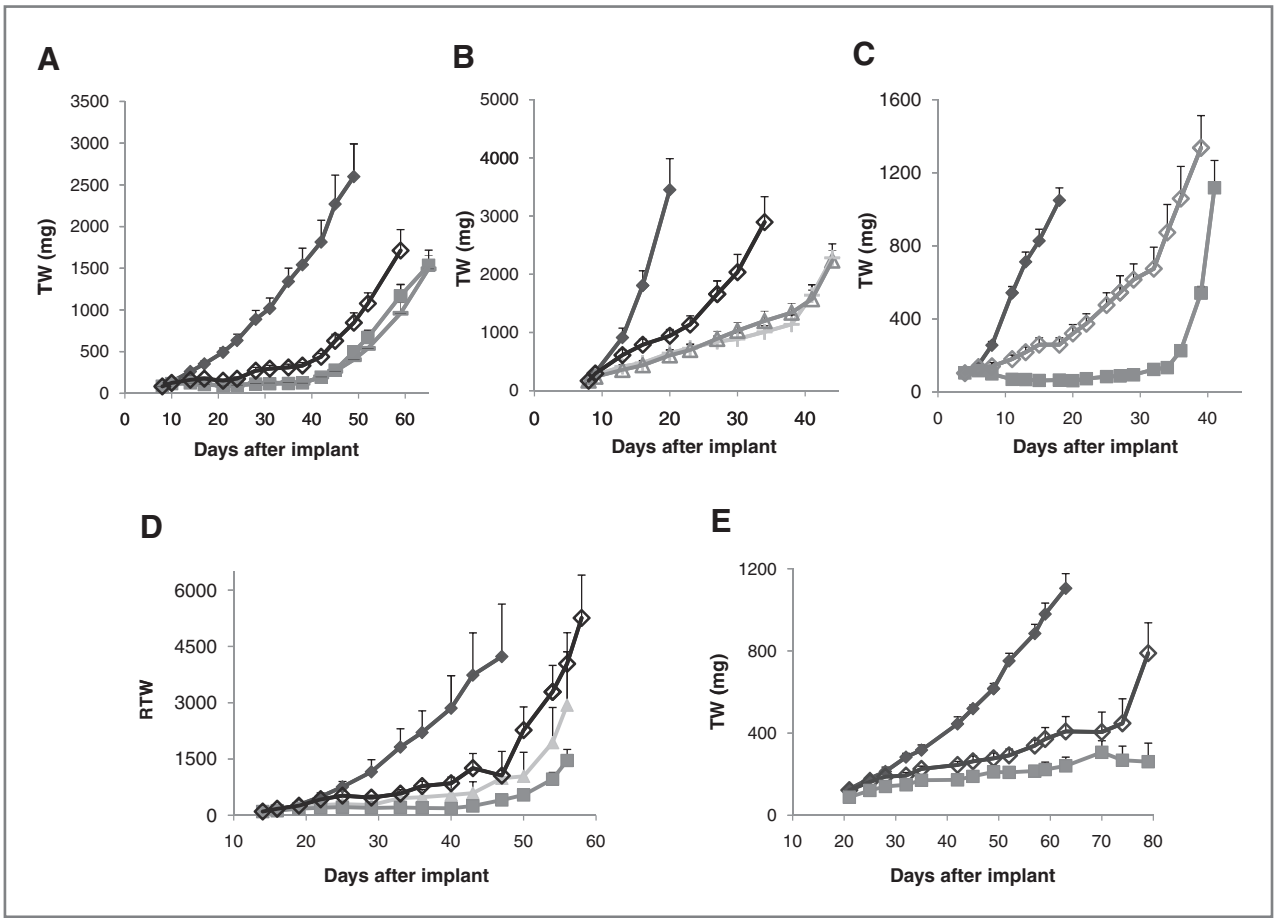

Figure 2. Tumor growth inhibition after treatment with E-3810. The antitumor activity of E-3810 was tested in HT-29 colon cancer (A), in A2780 tumor xenograft (B), in RXF393 (C), in A498 (D), and in SKN12I (E) renal xenografts. All tumors were transplanted subcutaneously and when the masses reached 100 to 150 mg, mice were randomized to receive daily for 30 consecutive days vehicle (♦), E-3810 10 mg/kg (▲), 15 mg/kg (+), 20 mg/kg (■), 30 mg/kg (Δ), 40 mg/kg (–), and sunitinib 40 mg/kg (◇). Panel D reports the relative tumor weight (RTW).

phosphorylation, a downstream marker of both VEGF and FGF signaling, was also inhibited. In NIH3T3 cells, PDGFR auto-phosphorylation was inhibited only at E-3810 concentrations in the μM range (Supplementary Fig. S1C). Consistent with the inhibitory activity of VEGFR and FGFR auto-phosphorylation, E-3810 potently inhibited VEGF and bFGF-stimulated HUVEC proliferation with IC_{50} of 40 and 50 nM, respectively. We then tested E-3810 activity *in vitro* on different human cancer cell lines and, as opposed to HUVEC system, μM concentrations were needed to inhibit cell growth in nonligand-dependent conditions (Supplementary Fig. S1D).

In vivo studies

Antiangiogenetic effect of E-3810. The effect of E-3810 on angiogenesis was studied in an *in vivo* model of vessel formation induced by bFGF in a Matrigel plug injected subcutaneously in mice. bFGF embedded in the plug induced a strong angiogenic response, with a 2- to 3-fold increase ($P < 0.01$) in hemoglobin content compared with plugs containing Matrigel alone (Supplementary Fig. S2). E-3810, at oral dosing of 20 mg/kg for 7 consecutive days, completely inhibited ($P < 0.01$) the bFGF induced angiogenic response compared with the response in vehicle-treated mice (Supplementary Fig. S2).

E-3810 efficacy in human tumor xenograft models. The *in vivo* efficacy of E-3810 was studied on a broad panel of human tumor xenografts and in different experimental conditions (Figs. 2 and 3 and Table 2). The activity of sunitinib and brivanib at their reported optimal doses (26, 30–32) is also presented (Figs. 2 and 3). E-3810 showed a broad spectrum of activity, being active in all the xenografts tested (HT29 colon carcinoma, A2780 ovarian carcinoma, A498, SN12K1, and RXF393 renal carcinomas) with dose-dependent inhibition of tumor growth (Fig. 2, Table 2, and data not shown). The optimal dose-schedule was defined as 20 mg/kg given daily by mouth (p.o.) for 30 days; this schedule caused less than 10% weight loss (Supplementary Fig. S3). E-3810 significantly delayed growth during treatment, but tumors resumed their growth when treatment was suspended (Fig. 2); in a few cases, tumor regression was observed (Fig. 2C). These effects were similar to those observed with sunitinib tested at its optimal dose (40 mg/kg daily; Fig. 2).

Published OnlineFirst January 6, 2011; DOI: 10.1158/0008-5472.CAN-10-2700

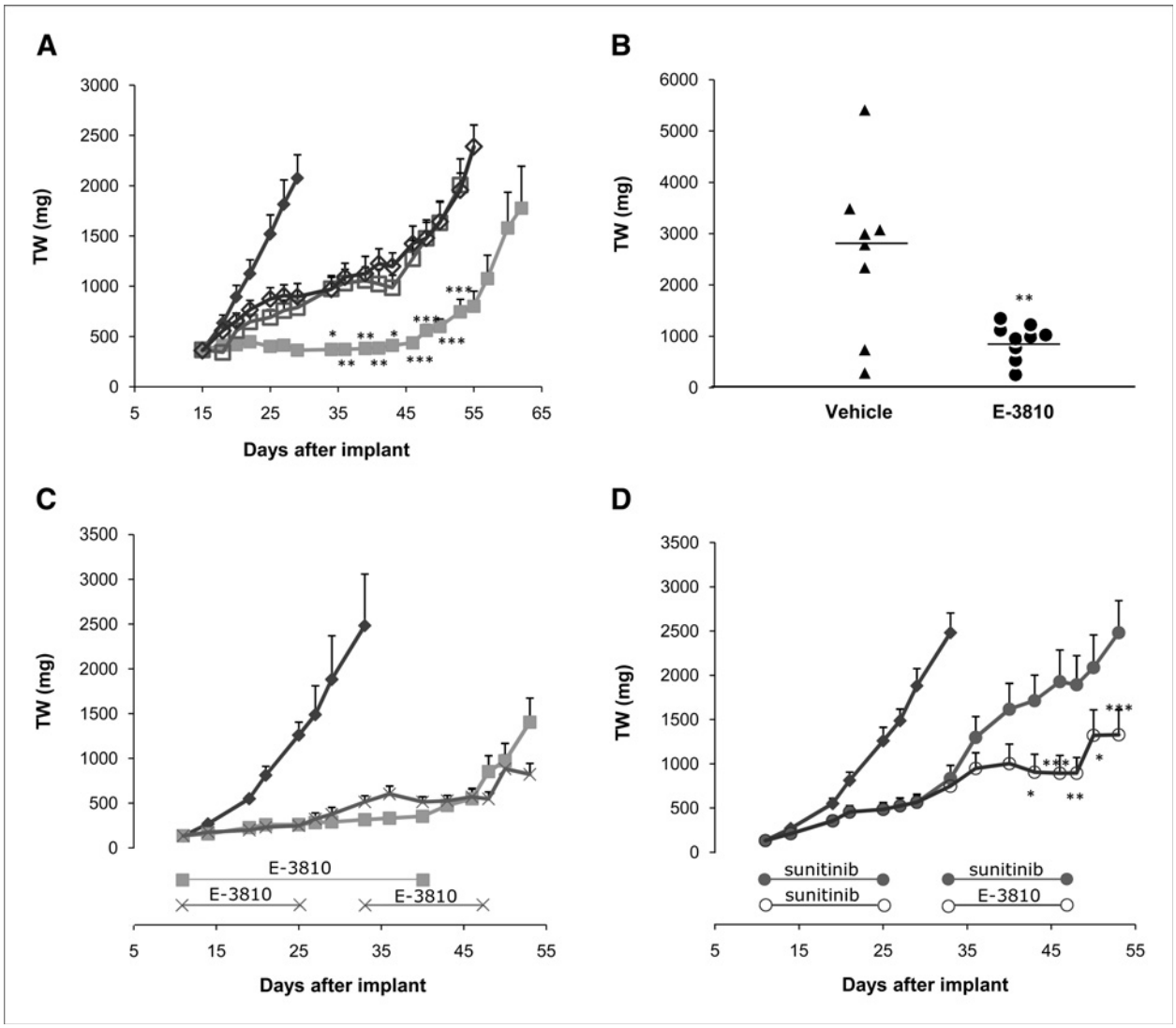

Figure 3. Antitumor activity of E-3810 in mice bearing A498 tumor xenograft. A, A498 tumors were allowed to grow to 400 mg. Mice were randomized to receive: vehicle (♦), E-3810 20 mg/kg every day for 30 days (■), brivanib 100 mg/kg every day for 30 days (□), and sunitinib 40 mg/kg every day for 30 days (◇). *, $P < 0.01$; **, $P < 0.05$; ***, $P < 0.005$. B, A498 tumor cells were orthotopically transplanted in the kidney of nude mice. After 17 days, mice were randomized to receive vehicle (▲) or E-3810 (●) 20 mg/kg every day for 30 days. At the end of the treatment mice were killed and kidneys were harvested and weighed. C, mice transplanted with A498 tumors were randomized when the tumor reached 100 to 150 mg to receive vehicle (♦), E-3810 20 mg/kg every day for 30 days, (■), or E-3810 20 mg/kg every day for 15 days x2 after a 1-week rest (x). D, mice transplanted with A498 tumors were randomized when the tumors reached 100 to 150 mg to receive vehicle (♦), sunitinib 40 mg/kg every day for 15 days × 2 cycles after a 1-week rest (●), and sunitinib 40 mg/kg every day for 15 days followed by E-3810 20 mg/kg every day for 15 days after a 1-week rest (○). *, $P < 0.01$, **, $P < 0.05$, and ***, $P < 0.005$.

The A498 renal cancer xenograft model was used to study the antitumor activity of E-3810 in specific settings (Fig. 3). E-3810 was very effective in advanced disease, when treatment started at a tumor size of approximately 400 to 500 mg (Fig. 3A). Similarly to the early stage setting, stabilization was observed for the whole duration of treatment but tumors resumed their growth on drug withdrawal. In this late-stage setting, the comparison with brivanib, a dual VEGFR and FGFR inhibitor, indicated better activity of E-3810 both in terms of tumor stabilization and tumor growth delay [tumor growth inhibition (TGI) rate of 83%, 62%, and 56% and $T - C$ to reach 1 g in 34.8, 14.6, and 12.6 days, respectively in E-3810-, brivanib-, and sunitinib-treated animals; Fig. 3A]. We also tested the activity of E-3810 on A498 transplanted orthotopically in the kidney of nude mice, to reproduce the organ environment of the tumor of origin better (Fig. 3B). Treatment started on day 17 when the tumors in the kidney were already detectable (data not shown) and continued for 30 days at the schedule of 20 mg/kg daily p.o. At the end of treatment, mice were killed and their kidneys were removed and weighed. E-3810 significantly ($P < 0.05$) inhibited tumor growth (mean ± SD kidney weights respectively, 2,654 ± 1,603 mg and 914 ± 345 mg in controls and treated mice); kidneys of non–tumor-bearing mice weighed about 157 mg.

Published OnlineFirst January 6, 2011; DOI: 10.1158/0008-5472.CAN-10-2700

Table 2. Daily oral treatment with E-3810 inhibits the growth of different human tumor xenografts

Xenograft	Tumor type	Initial tumor volume (mg)	Dose (mg/kg/d)	%TGI (d)	*T* − *C* (d)
HT-29	Colon	100-150	20	92 (38)	27.4*/28**
			40	92 (38)	29*/30**
A2780	Ovarian	100-150	15	81 (20)	16*
			30	82(20)	20*
A498	Renal	100-150	10	84 (43)	21*
			20	91(40)-93 (40)	27*
		350-400	20	82 (29)	35*/29**
SN12KI	Renal	100-150	20	81 (74)	29**
RXF393	Renal	100-150	20	94 (20)	23*/28**

NOTE: E-3810 was given p.o. at the indicated doses for 30 consecutive days, starting when tumor masses reached 100 to 150 mg or 350 to 400 mg as indicated in the text. %TGI, tumor growth inhibition; *T* − *C* (d), difference between treated and control mice in time to reach 500 mg (*) or 1,000 mg (**).

Finally, we investigated the activity of E-3810 given continuously or intermittently. The antitumor activities were comparable at the optimal dose schedule (20 mg/kg daily for 30 days) or in 2 cycles (20 mg/kg daily for 15 days, twice, with 1 week's interruption; Fig. 3C), with similar tumor responsiveness to the first and second cycle of therapy. When A498 tumor bearing mice were treated with sunitinib for 15 days at the optimal reported dose (40 mg/kg daily) then, after 1 week of suspension, retreated with sunitinib or E-3810 for a second cycle, tumor growth was again stabilized by E-3810 but continued under sunitinib (Fig. 3D). These data suggest E-3810 is active in tumors resistant to other antiangiogenic drugs.

E-3810 pharmacokinetics. In pharmacokinetic experiments (Supplementary Fig. 4), E-3810 showed a good oral bioavailability. The kinetic profile in nude mice indicated a low-to-moderate clearance and a high volume of distribution. The terminal half-life was about 4 hours and comparable after oral and i.v. administration (Supplementary Fig. 4A). The drug systemic exposure was proportional to the dose and its kinetic did not change after repeated daily doses (Supplementary Fig. 4B and C). After single and repeated doses, E-3810 was measurable in tumors, with concentrations higher than in plasma (Supplementary Fig. 4D).

In vivo *effects on tumor perfusion and permeability detected by DCE-MRI.* Figure 4A shows regions of interest (ROI), namely the tumor rim and the tumor core, superimposed on an anatomic image. The signal enhancement at $T = 0$, 1, and 2, defined as % Enh (t) = 100 × (signal at time t post CA injection − signal preinjection)/signal preinjection, was calculated for the 2 ROIs and for vehicle and E-3810 treated animals. As the % Enh (t) is proportional to the total concentration of CA in the tissue at time t, the analysis indicates a significant reduction of perfusion in E-3810 treated tumors compared with baseline values and vehicle-treated controls, already after only 5 days. To quantify this reduction, the median of the initial area under the time–signal enhancement curve (IAUC), defined over the first 10 minutes after injection of contrast medium ($IAUC_{10}$), was calculated and the results are plotted in Fig. 4B. $IAUC_{10}$ values differed significantly in control and E-3810 groups.

A 2-compartment model was used to fit the DCE series and extract, voxel-wise, the fractional plasma volume (fPV; i.e., the fPV of the voxel occupied by plasma) and the kinetic transfer constant K^{trans} between the 2 compartments. The latter reflects the permeability of the tumor capillaries to the molecule used as CA (in our case the albumin-bound form of B22956/1). Median pixel values were calculated for each ROI from the fPV and K^{trans} parametric images. Results are summarized in Supplementary Table S2. There was a general reduction in the fPV of E-3810 treated mice (though significant only at T1), but no considerable differences in the permeability to B22956/1.

E-3810 induces vascular regression in human renal carcinoma xenografts. The specific effects of E-3810 on tumor vasculature from vehicle- and drug-treated animals were examined using CD31 immunohistochemistry on A498 tumor xenografts (Fig. 5, left). Vascular density in control A498 tumors did not change significantly during the 12 days of growth (data not shown). In contrast, there was an 80% reduction of vascular density in E-3810–treated tumors compared to the time-matched controls. In addition, there was a decrease in the deposition of collagen IV, detected after immunostaining for murine collagen IV (Fig. 5, middle), and an increase in tumor necrosis assessed using H&E stained sections (Fig. 5, right). All these data parallel the results with bFGF-induced angiogenesis in Matrigel plugs (Supplementary Fig. S2) and those on tumor perfusion by DCE-MRI (Fig. 4), corroborating the strong antiangiogenic effect of E-3810.

Discussion

The aim of this study was to characterize the pharmacologic profile of E-3810, a dual inhibitor of VEGFR and FGFR tyrosine kinases. The compound was very active in biochemical assays, inhibiting the kinase activity of VEGFR-1, -2, and -3; FGFR-1 and -2; and CSF-1R at nanomolar concentrations, but with much less potency on PDGFR α and β. Our *in vitro*

Published OnlineFirst January 6, 2011; DOI: 10.1158/0008-5472.CAN-10-2700

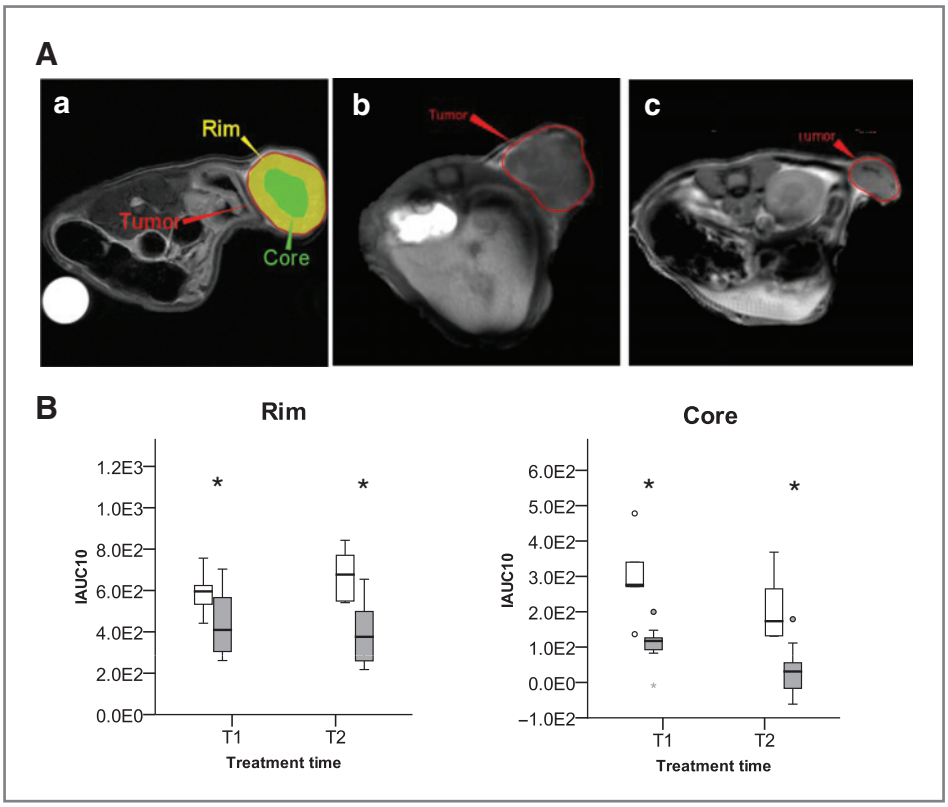

Figure 4. Effects of E-3810 on tumor perfusion evaluated by DCE-MRI in A498 tumor bearing mice. A, illustrative MRI images. a, ROIs used for the image analysis; the red line outlines the whole tumor region, yellow and green areas represent respectively the tumor rim (a 1- to 1.5-mm-thick band in the tumor border) and core (center of the tumor). b and c, average images of the DCE series of 1 control and 1 treated animal, respectively. Images were taken at treatment time T2. B, box-plot of the $IAUC_{10}$ in tumor rim and core. $IAUC_{10}$ is the initial area under the signal enhancement curve calculated from the first 10 minutes of the DCE-MRI signal time course. The value of $IAUC_{10}$ is proportional to the amount of blood flow through the tumor during the first 10 minutes after contrast agent injection. Boxes refer to the control group (□) and E-3810 treated group (■). *, $P < 0.05$ (Mann–Whitney U test); anomalous data points are plotted with a dot or a star.

and *in vivo* data are consistent with a key role of the inhibition of VEGFR and FGFR in the mode of action of E-3810, even if we cannot rule out the possibility that other important kinases for tumor cell growth could be affected by E-3810. *In vitro* E-3810 inhibits the VEGF- and bFGF-dependent proliferation and the signaling transduction pathways elicited by VEGF and bFGF ligands binding to their cognate receptors in HUVEC cells in the nanomolar range. Much higher concentrations (μM) were needed to interfere *in vitro* with the growth of different cell lines in nonligand stimulated conditions, suggesting that the drug effect on tumor cells occurs at quite high concentrations and that the drug's primary effect is inhibition of VEGF and FGF signaling pathways, which are pivotal in the proliferation and survival of endothelial and stromal cells. *In vivo* 7 days of treatment with E-3810 completely inhibited the FGF-induced angiogenesis in an implanted Matrigel plug in mice; E-3810 treatment significantly reduced tumor vessel density in treated tumors (as assessed by the decrease in CD31 staining), increasing in the percentage of tumor necrosis and changing the composition of tumor stroma (with a decrease in collagen IV content).

These findings were corroborated by DCE-MRI analysis, which showed that E-3810 reduced the tumor distribution of the CA, already after only 5 days of treatment. This MRI evidence suggests that, as for other inhibitors, the antiangiogenic response to E-3810 can be monitored *in vivo*, with widely available technology and an established method suitable for the clinical setting.

All the effects indicate a strong antiangiogenic effect of E-3810 that is likely to greatly contribute to its potent antitumor effect in the human xenografts tested, encompassing ovarian, renal, and colorectal carcinomas. E-3810's main effect was tumor stabilization, with regression in some experimental settings. These results are consistent with the activity reported for other antiangiogenic compounds in preclinical systems (33, 34), although E-3810's antitumor effect in our experimental human xenografts was always equal, when not superior, to sunitinib and brivanib used at their optimal dose schedules (26, 35). The drug also showed significant antitumor activity in RXF393 xenografts grown orthotopically in the kidney of nude mice, reproducing the site of tumor origin. In addition, the compound displayed a good pharmacokinetic profile: complete oral bioavailability, terminal half-life about 4 hours, and systemic exposure proportional to the dose with no accumulation after daily treatment. In addition, the observed high activity of E-3810 in inhibiting in biochemical assay CSF-R1, could suggest a modulation of tumor-associated macrophage (TAM) function. It is well known that CSF is the main growth factor responsible for the survival, proliferation, differentiation, and chemotaxis of mononuclear phagocytes, such as macrophages (36). CSF-1 has been shown to block the maturation of dentritic cells in tumors in such a way that they are unable to present antigens and promote immuno-suppresed trophic TAMs, with a less inflammatory and proangiogenic phenotype (37, 38). The interference with these processes might contribute to the drug's antitumor effects.

In all the experimental settings, however, tumor growth resumed after drug withdrawal, suggesting that continuous target inhibition is needed. However, tumors responded to a second cycle of E-3810 to the same extent as to the first cycle

Published OnlineFirst January 6, 2011; DOI: 10.1158/0008-5472.CAN-10-2700

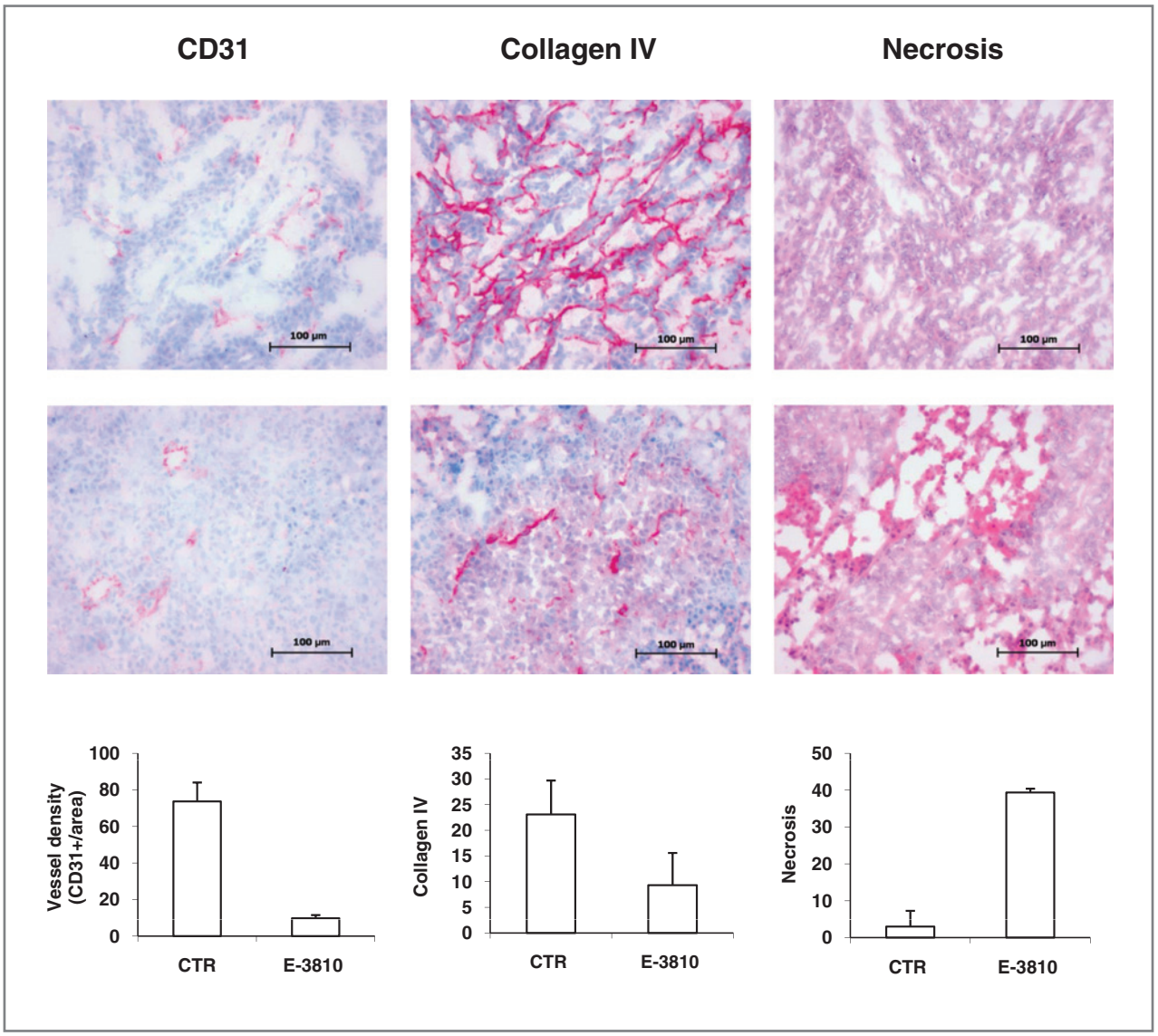

Figure 5. Immunohistochemistry of A498 tumors treated with E-3810 or not. Immunohistochemical analysis of tumor vessel density (CD31; left), tumor stroma (collagen IV; middle), and necrosis (right) in A498 tumors from control (top) and E-3810–treated (middle) animals. Effects are quantified in the bottom panels. Data are mean ± SD.

(Fig. 3C) suggesting that tumor regrowth upon treatment withdrawal is not associated with the development of resistance. In addition, tumors initially treated with sunitinib then treated with a second cycle of sunitinib or E-3810 were resistant to sunitinib, but sensitive to E-3810. These data need to be confirmed in other experimental settings but they do suggest that the mechanisms underlying resistance to sunitinib can be overridden by E-3810.

The mechanisms for the development of resistance to VEGF pathway inhibitors in tumors are far from fully elucidated (14, 16, 17), but various alternative angiogenic signaling pathways have been reported (39–41). For example, placental growth factor (PIGF), a member of the VEGF family that specifically binds VEGFR1, was up-regulated in patients treated with antiangiogenic agents (10, 42). PIGF mRNA was upregulated in mice treated with anti-VEGFR2 antibodies (40), and treatment with anti-PIGF antibody had an additive effect in slowing tumor growth when combined with anti-VEGFR-2 antibody (18). FGFs have also been reported to sustain angiogenesis independently of VEGF (43, 44). In a RIP-tag model, FGF1 and FGF2 were upregulated in tumors relapsed after treatment with the anti-VEGFR antibody DC101 (39). Inhibition of the FGF/FGFR pathway with a FGF-trap (FGFR-Fc fusion peptide) in this experimental model slowed tumor growth and attenuated tumor angiogenesis. FGF2 was increased in the blood of patients relapsed after treatment with VEGFR inhibitors (10), suggesting its role in acquired resistance.

The resistance to sunitinib retreatment we observed in A498 tumors might be due to a shift from VEGF/VEGFR to a FGF/FGFR driven angiogenesis, which can be countered

Published OnlineFirst January 6, 2011; DOI: 10.1158/0008-5472.CAN-10-2700

by E-3810, as it is a more potent and specific inhibitor of FGFRs than sunitinib (35). In biochemical assays FGFR-1 and -2 were inhibited by E-3810 at the same nanomolar concentrations of VEGFRs, whereas higher concentrations are needed for sunitinib. Studies are ongoing to prove this.

Besides the role of the FGF/FGFR pathway in driving tumor angiogenesis, deregulation by activating mutations or ligand/receptor overexpression may also lead to tumor development and maintenance (19, 45, 46). Thus, a dual inhibitor of VEGFR and FGFR is potentially able to inhibit both proangiogenic pathways and the FGF/FGFR signal required for the growth and survival of cancer cells. Our data clearly show that E-3810 is a strong inhibitor of angiogenesis, but in tumor cells highly dependent on FGF/FGFR it may also have some direct antiproliferative or cytotoxic effect. If this is the case, the dual mechanism of drug action should result in a better clinical response in patients whose tumor growth depends on FGF/FGFR.

Overall, this study defines E-3810 as a small tyrosine kinase molecule with a potent antiangiogenic effect, a favorable pharmacokinetic profile, a broad spectrum of antitumor activity, and good tolerability, providing a strong rationale for its clinical investigation.

Disclosure of Potential Conflicts of Interest

No potential conflicts of interest were disclosed.

Acknowledgments

Contributions from FP7-Adamant and Cariplo Foundation are acknowledged. We thank K. Bonezzi for technical assistance in the Matrigel Study and E. Micotti for technical assistance in the MRI experiments.

Grant Support

This research was supported by a research grant from E.O.S. S.p.A.

The costs of publication of this article were defrayed in part by the payment of page charges. This article must therefore be hereby marked *advertisement* in accordance with 18 U.S.C. Section 1734 solely to indicate this fact.

Received July 26, 2010; revised October 26, 2010; accepted December 4, 2010; published OnlineFirst January 6, 2011.

References

1. Kerbel RS. Tumor angiogenesis. N Engl J Med 2008;358:2039–49.
2. Bergers G, Benjamin LE. Tumorigenesis and the angiogenic switch. Nat Rev Cancer 2003;3:401–10.
3. Ferrara N, Kerbel RS. Angiogenesis as a therapeutic target. Nature 2005;438:967–74.
4. Hanahan D, Weinberg RA. The hallmarks of cancer. Cell 2000;100:57–70.
5. McDermott DF, George DJ. Bevacizumab as a treatment option in advanced renal cell carcinoma: an analysis and interpretation of clinical trial data. Cancer Treat Rev 2010;36:216–23.
6. Crawford Y, Ferrara N. VEGF inhibition: insights from preclinical and clinical studies. Cell Tissue Res 2009;335:261–9.
7. Chung AS, Lee J, Ferrara N. Targeting the tumour vasculature: insights from physiological angiogenesis. Nat Rev Cancer 2010;10:505–14.
8. Ivy SP, Wick JY, Kaufman BM. An overview of small-molecule inhibitors of VEGFR signaling. Nat Rev Clin Oncol 2009;6:569–79.
9. Hurwitz H, Fehrenbacher L, Novotny W, Cartwright T, Hainsworth J, Heim W, et al. Bevacizumab plus irinotecan, fluorouracil, and leucovorin for metastatic colorectal cancer. N Engl J Med 2004;350:2335–42.
10. Batchelor TT, Sorensen AG, di Tomaso E, Zhang WT, Duda DG, Cohen KS, et al. AZD2171, a pan-VEGF receptor tyrosine kinase inhibitor, normalizes tumor vasculature and alleviates edema in glioblastoma patients. Cancer Cell 2007;11:83–95.
11. Ma J, Waxman DJ. Combination of antiangiogenesis with chemotherapy for more effective cancer treatment. Mol Cancer Ther 2008;7:3670–84.
12. Shojaei F, Ferrara N. Antiangiogenic therapy for cancer: an update. Cancer J 2007;13:345–8.
13. Saltz LB, Lenz HJ, Kindler HL, Hochster HS, Wadler S, Hoff PM, et al. Randomized phase II trial of cetuximab, bevacizumab, and irinotecan compared with cetuximab and bevacizumab alone in irinotecan-refractory colorectal cancer: the BOND-2 study. J Clin Oncol 2007;25:4557–61.
14. Bergers G, Hanahan D. Modes of resistance to anti-angiogenic therapy. Nat Rev Cancer 2008;8:592–603.
15. Grepin R, Pages G. Molecular mechanisms of resistance to tumour anti-angiogenic strategies. J Oncol 2010;2010:835680.
16. Abdollahi A, Folkman J. Evading tumor evasion: current concepts and perspectives of anti-angiogenic cancer therapy. Drug Resist Updat 2010;13:16–28.
17. Eikesdal HP, Kalluri R. Drug resistance associated with antiangiogenesis therapy. Semin Cancer Biol 2009;19:310–7.
18. Crawford Y, Ferrara N. Tumor and stromal pathways mediating refractoriness/resistance to anti-angiogenic therapies. Trends Pharmacol Sci 2009;30:624–30.
19. Knights V, Cook SJ. De-regulated FGF receptors as therapeutic targets in cancer. Pharmacol Ther 2010;125:105–17.
20. Korc M, Friesel RE. The role of fibroblast growth factors in tumor growth. Curr Cancer Drug Targets 2009;9:639–51.
21. Acevedo VD, Ittmann M, Spencer DM. Paths of FGFR-driven tumorigenesis. Cell Cycle 2009;8:580–8.
22. Elbauomy Elsheikh S, Green AR, Lambros MB, Turner NC, Grainge MJ, Powe D, et al. FGFR1 amplification in breast carcinomas: a chromogenic in situ hybridisation analysis. Breast Cancer Res 2007;9:R23.
23. Eswarakumar VP, Lax I, Schlessinger J. Cellular signaling by fibroblast growth factor receptors. Cytokine Growth Factor Rev 2005;16:139–49.
24. Turner N, Grose R. Fibroblast growth factor signalling: from development to cancer. Nat Rev Cancer 2010;10:116–29.
25. Pond AC, Herschkowitz JI, Schwertfeger KL, Welm B, Zhang Y, York B, et al. Fibroblast growth factor receptor signaling dramatically accelerates tumorigenesis and enhances oncoprotein translation in the mouse mammary tumor virus-Wnt-1 mouse model of breast cancer. Cancer Res 2010;70:4868–79.
26. Bhide RS, Lombardo LJ, Hunt JT, Cai ZW, Barrish JC, Galbraith S, et al. The antiangiogenic activity in xenograft models of brivanib, a dual inhibitor of vascular endothelial growth factor receptor-2 and fibroblast growth factor receptor-1 kinases. Mol Cancer Ther 2010;9:369–78.
27. Naumova E, Ubezio P, Garofalo A, Borsotti P, Cassis L, Riccardi E, et al. The vascular targeting property of paclitaxel is enhanced by SU6668, a receptor tyrosine kinase inhibitor, causing apoptosis of endothelial cells and inhibition of angiogenesis. Clin Cancer Res 2006;12:1839–49.
28. de Haen C, Anelli PL, Lorusso V, Morisetti A, Maggioni F, Zheng J, et al. Gadocoletic acid trisodium salt (b22956/1): a new blood pool magnetic resonance contrast agent with application in coronary angiography. Invest Radiol 2006;41:279–91.
29. Brasch R, Pham C, Shames D, Roberts T, van Dijke K, van Bruggen N, et al. Assessing tumor angiogenesis using macromolecular MR imaging contrast media. J Magn Reson Imaging 1997;7:68–74.

Published OnlineFirst January 6, 2011; DOI: 10.1158/0008-5472.CAN-10-2700

30. Huynh H, Ngo VC, Fargnoli J, Ayers M, Soo KC, Koong HN, et al. Brivanib alaninate, a dual inhibitor of vascular endothelial growth factor receptor and fibroblast growth factor receptor tyrosine kinases, induces growth inhibition in mouse models of human hepatocellular carcinoma. Clin Cancer Res 2008;14:6146–53.
31. Cumashi A, Tinari N, Rossi C, Lattanzio R, Natoli C, Piantelli M, et al. Sunitinib malate (SU-11248) alone or in combination with low-dose docetaxel inhibits the growth of DU-145 prostate cancer xenografts. Cancer Lett 2008;270:229–33.
32. Abrams TJ, Murray LJ, Pesenti E, Holway VW, Colombo T, Lee LB, et al. Preclinical evaluation of the tyrosine kinase inhibitor SU11248 as a single agent and in combination with "standard of care" therapeutic agents for the treatment of breast cancer. Mol Cancer Ther 2003;2:1011–21.
33. Ellis LM, Hicklin DJ. VEGF-targeted therapy: mechanisms of anti-tumour activity. Nat Rev Cancer 2008;8:579–91.
34. Bagri A, Berry L, Gunter B, Singh M, Kasman I, Damico LA, et al. Effects of treatment duration with anti-VEGF antibodies on tumor growth, regrowth, and efficacy. Clin Cancer Res 2010;16:3887–900.
35. Mendel DB, Laird AD, Xin X, Louie SG, Christensen JG, Li G, et al. In vivo antitumor activity of SU11248, a novel tyrosine kinase inhibitor targeting vascular endothelial growth factor and platelet-derived growth factor receptors: determination of a pharmacokinetic/pharmacodynamic relationship. Clin Cancer Res 2003;9:327–37.
36. Hamilton JA. Colony-stimulating factors in inflammation and autoimmunity. Nat Rev Immunol 2008;8:533–44.
37. Pollard JW. Tumour-educated macrophages promote tumour progression and metastasis. Nat Rev Cancer 2004;4:71–8.
38. Mantovani A, Sica A. Macrophages, innate immunity and cancer: balance, tolerance, and diversity. Curr Opin Immunol 2010;22:231–7.
39. Casanovas O, Hicklin DJ, Bergers G, Hanahan D. Drug resistance by evasion of antiangiogenic targeting of VEGF signaling in late-stage pancreatic islet tumors. Cancer Cell 2005;8:299–309.
40. Fischer C, Jonckx B, Mazzone M, Zacchigna S, Loges S, Pattarini L, et al. Anti-PlGF inhibits growth of VEGF(R)-inhibitor-resistant tumors without affecting healthy vessels. Cell 2007;131:463–75.
41. Ferrara N. Pathways mediating VEGF-independent tumor angiogenesis. Cytokine Growth Factor Rev 2010;21:21–6.
42. Motzer RJ, Michaelson MD, Redman BG, Hudes GR, Wilding G, Figlin RA, et al. Activity of SU11248, a multitargeted inhibitor of vascular endothelial growth factor receptor and platelet-derived growth factor receptor, in patients with metastatic renal cell carcinoma. J Clin Oncol 2006;24:16–24.
43. Cao Y, Cao R, Hedlund EM. Regulation of tumor angiogenesis and metastasis by FGF and PDGF signaling pathways. J Mol Med 2008;86:785–9.
44. Alessi P, Leali D, Camozzi M, Cantelmo A, Albini A, Presta M. Anti-FGF2 approaches as a strategy to compensate resistance to anti-VEGF therapy: long-pentraxin 3 as a novel antiangiogenic FGF2-antagonist. Eur Cytokine Netw 2009;20:225–34.
45. Bernard-Pierrot I, Brams A, Dunois-Larde C, Caillault A, Diez de Medina SG, Cappellen D, et al. Oncogenic properties of the mutated forms of fibroblast growth factor receptor 3b. Carcinogenesis 2006;27:740–7.
46. Beenken A, Mohammadi M. The FGF family: biology, pathophysiology and therapy. Nat Rev Drug Discov 2009;8:235–53.

Cancer Research
The Journal of Cancer Research (1916–1930) | The American Journal of Cancer (1931–1940)

AACR American Association for Cancer Research

E-3810 Is a Potent Dual Inhibitor of VEGFR and FGFR that Exerts Antitumor Activity in Multiple Preclinical Models

Ezia Bello, Gennaro Colella, Valentina Scarlato, et al.

Cancer Res 2011;71:1396-1405. Published OnlineFirst January 6, 2011.